Earthquakes and Structures, *Vol. 18, No. 3 (2020) 275-284*
DOI: https://doi.org/10.12989/eas.2020.18.3.275

Experimental and numerical investigation of wire rope devices in base isolation systems

Andrea Calabrese[1], Mariacristina Spizzuoco[*2], Daniele Losanno[2] and Arman Barjani[1]

[1]*Dept. of Civil Engineering & Construction Engineering Management, California State Univ. Long Beach, Long Beach, CA, USA*
[2]*Department of Structures for Engineering and Architecture, University of Naples Federico II, Via Claudio 21, Naples, Italy*

(*Received January 30, 2019, Revised November 13, 2019, Accepted January 4, 2020*)

Abstract. The scope of this study is the comparison between experimental results of tests performed on a base isolated building using helical wire rope isolators (WRs), and results of Nonlinear Response History Analyses (NRHAs) performed using SAP 2000, a commercial software for structural analysis. In the first stage of this research, WRs have been tested under shear deformation beyond their linear range of deformation, and analytical models have been derived to describe the nonlinear response of the bearings under different directions of loading. On the following stage, shaking table tests have been carried out on a 1/3 scale steel model isolated at the base by means of curved surface sliders (CSS) and WRs. The response of the structure under ground motion excitation has been compared to that obtained using numerical analyses in SAP 2000. The feasibility of modelling the nonlinear behavior of the tested isolation layer using multilinear link elements embedded in SAP 2000 is discussed in this paper, together with the advantages of using WRs as supplemental devices for CSSs base isolated structures.

Keywords: seismic base isolation; wire rope isolators; shaking table tests; building structure

1. Introduction

The recentering capacity of a base isolation system is a fundamental characteristic of an isolation layer. This is the capacity of the isolation layer of recovering the undeformed configuration after a seismic event. The buildup of the residual displacement arising from a limited recentering capacity of the isolation system can adversely impact on the serviceability of the building and can jeopardize the displacement capacity of the isolation system in case of future earthquakes. The recentering of a base isolated structure is essential after pulse-like inputs such as the ones happening in near-field events, when large residual displacements can be expected (Liossatou and Fardis 2016, Ismail *et al*. 2016).

This research investigates the application of wire rope devices to enhance the recentering capacity of the curved surface sliders (CSSs) commonly adopted in building and bridges. CSSs were introduced in North America during the second half of the 80’s. When used in base isolation layers, CSSs support the structure’s weight to provide energy dissipation through friction, restoring forces, and to accommodate large lateral displacements. The concept investigated in this study is that (Ghalandari *et al*. 2018, Gesualdo and Lima 2012) of enhancing the recentering capability of an isolation system by using helical wire rope isolators (WRs). These devices help limiting the peak lateral displacement of the isolation layer thanks to a marked hardening response of the bearing under large levels of lateral deformation. WRs consist of a stainless steel cable wrapped in elicoidal coils and two retainer bars made of aluminum alloy. These devices have been widely used in electronic, air space and military applications. WRs have proved to be cost-effective, resistant against environmental and chemical agents, durable under elevated temperatures, and have proven to require limited maintenance (Cutchins *et al*. 1987, Yurdakul and Ates 2011). The vertical stiffness of these devices depends on their geometry. It decreases with their 'height to width' ratio, and with the coil’s diameter. Due to their limited vertical load capacity, the application of WRs to civil engineering constructions is practical only in case of lightweight structures. In WRs energy dissipation is due to the friction among the individual wires; the equivalent viscous damping ratio has been reported to increase with the vertical load (Vaiana *et al*. 2017a). A WR can be tuned to have a different response in the different directions of loading. For their vibration isolation and energy dissipation capacities, these bearings have been successfully adopted to isolate transformation open-air substation’s circuit breakers (Di Donna and Serino 2002, Serino *et al*. 1995) and high voltage electrical equipment, as discussed in a research work by Giannini *et al*. (2015). Viable applications of this technology to buildings and bridges include their installation in combination with other aseismic devices like CSSs. In this configuration, CSSs sustain the structure’s weight and accommodate any horizontal displacement, while WRs could be used to improve the recentering capacity of the system and its energy dissipation characteristics. WRs could also help providing a hardening response to the structure that can limit the peak displacement of the isolation system before failure of the sliding devices. CSSs have been widely

∗Corresponding author, Ph.D.
E-mail: spizzuoc@unina.it

http://www.techno-press.org/?journal=eas&subpage=7
ISSN: 2092-7614 (Print), 2092-7622 (Online)

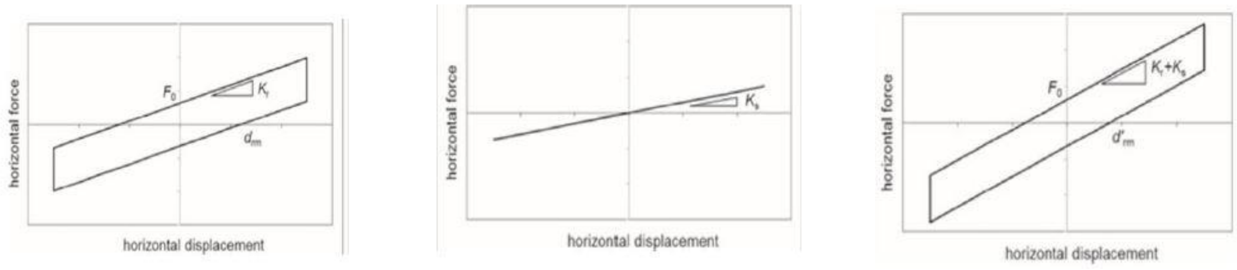

(a) (b) (c)

Fig. 1 Force–displacement cycles, along horizontal direction, of (a) a CSS having parameters F_0 and K_r, (b) a WR having lateral stiffness K_s, (c) a system obtained by connecting in parallel a CSS and a WR

adopted in buildings and bridges because of their relative low cost. The main advantage of using these bearings for base isolation is that the vibration period of a CSSs isolated structure is nearly independent of the structural mass and it only depends on the radius of curvature of the isolators. Using CSSs, a large displacement capacity of the isolation layer can be simply achieved by increasing the dimension of the sliding surface. The main drawback of CSSs include the variability of their response due to the environment (e.g., humidity for materials containing polyamide, and temperature (Dolce *et al*. 2005, Quaglini *et al*. 2012), and the vulnerability of the thermoplastic friction materials used for the sliding pads to aging, pollution, and wear. In CSSs, energy is dissipated trough friction at the interface of the concave surface and the sliding pad. In devices with a large coefficient of friction, large residual displacements can be expected. In addition, the static friction coefficient is higher than that dynamic one. When the structure remains at rest after a seismic excitation, the static friction is opposing to the recentering motion. Energy dissipation trough friction of the base isolation system is therefore not always ideal. The concept of using WRs in combination with CSSs seem to have many advantages: (i) WRs can provide an additional source of energy dissipation, hardening response and restoring force to a fraction of the cost of other aseismic devices; (ii) they can be easily installed below an existing structure, when the retrofit of an existing base isolated building is needed; (iii) a different response of the bearings can be defined for each direction of loading. The force displacement response of CSSs is shown in Fig. 1. F0 is the characteristic strength proportional to the vertical load W through the friction coefficient μ. $Kr = W/Reff$ is the restoring stiffness that depends on the effective radius *Reff* of the curved surface (Hussaini *et al*. 1994, Quaglini *et al*. 2014, Cardone *et al*. 2015, Katsaras *et al*. 2008). While the radius of curvature of the bearing can be modified to improve the recentering capacity of the system, this modification has an impact on the period of vibration and the vertical displacement u when the maximum lateral deformation d is reached (see Fig. 2).

WRs adopted in CSSs base isolated buildings produce an extra horizontal restoring force, while limiting the residual and vertical displacements of the isolation layer. Fig. 1 presents the effect of WRs in terms of reduction of the static residual displacement. In particular, it can be easily determined that $d'_{rm} / d_{rm} = Kr / (K_r + K_s)$, where d_{rm} is the static residual displacement of a CSS and d'_{rm} is the static residual displacement for the CSS and WR combination. These residual displacements are shown in Fig. 1(a) and 1(c), respectively.

This paper demonstrates the applicability of multilinear models to predict the response of a base isolated structure using wire rope devices and friction isolators. In the first part of this work, analytical models have been developed to predict the stiffness of WRs as function of their geometry and material. The viability of using WRs in combination with CSSs (WRs+CSSs) is discussed in this paper on the basis of shaking table tests. A comparison is made between the response of a framed structure isolated at the base with WRs+CSSs, with CSSs only and when the same structure is fixed at the base. The scopes of this research include the following objectives:

• to verify the feasibility of adopting cost-effective WRs in combination with CSSs for base isolation of civil engineering structures;
• to validate the feasibility of using simple multilinear models to predict the dynamic response of a frame structure, isolated at the base with the novel BI system;
• to validate the effectiveness of using the hardening response of WRs to limit the peak lateral displacement of CSSs base isolated buildings.

2. Modelling of a wire rope isolator

A twisted helical-shape wire rope device (Fig. 3(a)) is composed of a single stranded cable and two retaining bars (Costello 1990, Demetriades *et al*. 1993, Spizzuoco *et al*. 2017). Each coil formed by the steel cable is characterized by two semi circumferences on either side of the mounting bars: the first half circle is in the vertical plane, while the second half circle lies in a plane inclined according a twist angle β with respect to the vertical one (Fig. 3(b)). The mechanical properties of the device are function of different parameters including the cable length, the coils' height and width, the cable lay or twist, the direction of the applied load, the number of strands and their geometry. Closed form solutions defining the stiffness of the bearing under tension/compression (T/C), roll (R) and shear (S) have been derived by the authors (Love 1927). These modes of deformation are defined in Fig. 4. A non-linear hysteretic behavior is exhibited by the WRs when deformed along

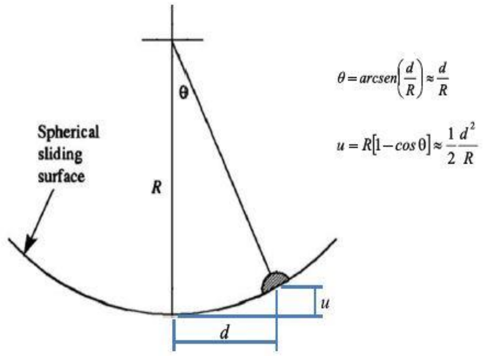

Fig. 2 Vertical and horizontal displacements of a CSS

each direction of loading. In the authors' work, only the linear response of the devices has been considered. Results of the analytical models are therefore applicable only to describe the stiffness of WRs under low levels of lateral deformation.

An object of the present study was to express the stiffness of a wire rope spring as function of its geometry and material characteristics. The model is based on the assumption that along three directions of loading, there is no interaction in the response of the bearing. The response of the isolator can therefore be modelled through three independent springs (Demetriades *et al.* 1993). This model also assumes that the individual wires in a WR cable do not interact with each other (*loose cable* assumption), so that the moment of inertia of the cross section of the single cable can be determined as sum of the inertia of each single wire. Some geometrical simplifications have been introduced as follows (Spizzuoco *et al.* 2017): the resultants of the external forces applied to the device are shifted from the axes of the retaining bars to their edges, so that each half loop of the coil is modeled as a semi circumference and the cable section retained within the bars is ignored (dimension *a* of Fig. 3(b)). For each direction of loading (Fig. 4), a spring model for a vertical loop has been formulated and solved in the tri-dimension (Love 1927, Belluzzi 1966, Den Hartog 1961).

The authors (Spizzuoco *et al.* 2017) have derived the expressions of the stiffness of one coil along the tension/compression, the shear, and the roll directions. The multiplication of the stiffness of a single coil ($k_{T/C}$, k_R, k_S) by the number of coils n_c provides an expression for the WR's total stiffness for each mode of deformation: $K_{T/C}=n_c\, k_{T/C}$, $K_R=n_c\, k_r$ and $K_s=n_c\, k_s$

The experimental stiffness (Spizzuoco *et al.* 2017) has been compared to the analytical one for the four WRs described in Table 1. For each deformation mode, the analytical stiffness was determined based on the *loose cable* assumption (Spizzuoco *et al.* 2017). Results are given in Tables 2 to 4. As clear from the tables, the maximum stiffness of the WRs is obtained in tension/compression. In these bearings, the roll and shear stiffness are generally similar. The ratio between the analytical and the experimental values belongs to the range 1.12 - 2.44 for the tension/compression mode, to the range 0.41 - 1.30 for the roll mode, and 0.43 - 1.21 for the shear mode.

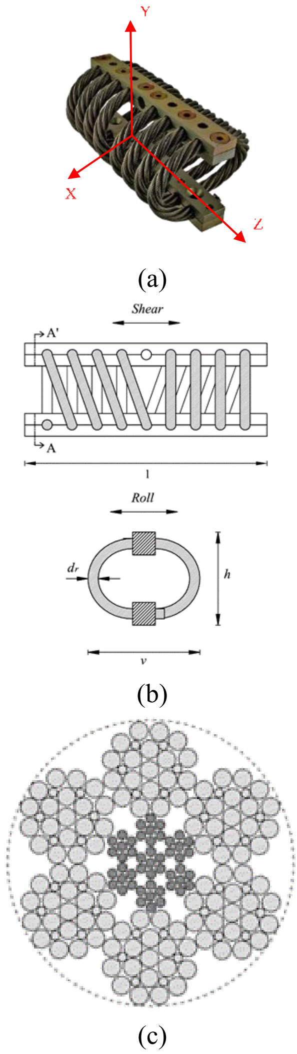

Fig. 3 (a) Cable and mounts of a wire rope; (b) usual helical configuration of the cable; (c) stranded cable's cross section

3. Isolation system including the assembly wire rope devices + sliding isolators

An assembly of sliding isolators and wire rope devices have been tested as base isolation system of a prototype-scaled building. This building has been part of many experimental programs at the Laboratory of the Department of Structures for Engineering and Architecture (DiSt) of the University of Naples Federico II (Italy) (e.g., Calabrese *et al.* 2015). The system's response under seismic excitation is discussed for the (a) fixed base structural configuration, (b) the structural mock-up isolated at the base by means of CSSs, and (c) the structure isolated at the base with CSSs+WRs. The seismic structural response in this configuration (a) was obtained performing time-history analyses in SAP2000, and compared against experimental results discussed in previous works (Calabrese *et al.* 2015).

3.1 Test setup

The steel superstructure is a 2-degrees-of-freedom system. The scale of the model is S_L = 1/3. The structure is

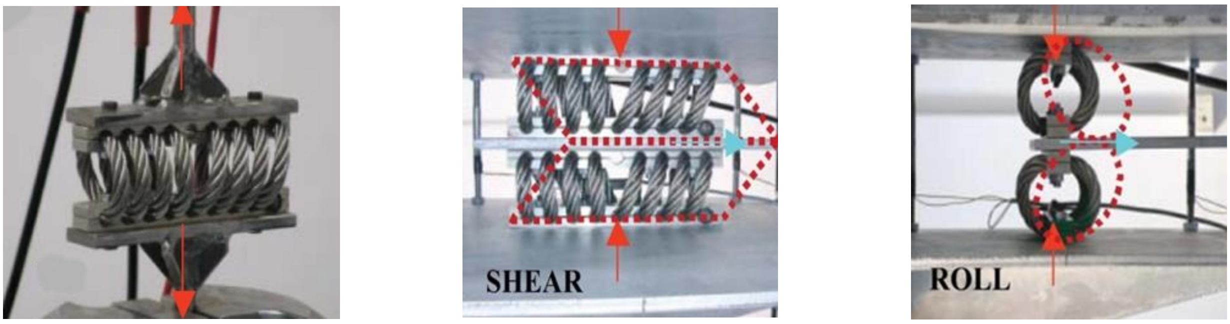

(a) (b) (c)

Fig. 4 Modes of deformation of the considered device: (a) 'tension/compression', (b) 'shear', (c) 'roll'

Table 1 Geometry of the wire rope isolators

		PWHS160	PWHS190	PWHS220	PWHS285
Number of coils	n_c	8	8	8	8
Coil diameter	D_c (mm)	68.5	75.5	122.5	131.5
Coil width	v (mm)	110	125	185	210
Coil height	h (mm)	100	105	150	185
Twist angle	β (rad)	0.315	0.400	0.333	0.380

Table 2 Experimental versus analytical results for the tension / compression stiffness

Stiffness	$K_{T/C}$ (N/mm)			
	PWHS160	PWHS190	PWHS220	PWHS285
Experimental	862	1429	1111	1423
Analytical (loose cable assumption) [Analytical / Experimental stiffness]	2104 [2.44]	2748 [1.92]	1241 [1.12]	2452 [1.72]

Table 3 Experimental versus analytical results for the roll stiffness

Stiffness	K_R (N/mm)			
	PWHS160	PWHS160	PWHS160	PWHS160
Experimental	278	278	278	278
Analytical (loose cable assumption) [Analytical / Experimental stiffness]	351 [1.26]	351 [1.26]	351 [1.26]	351 [1.26]

Table 4 Experimental versus analytical results for the shear stiffness

Stiffness	K_S (N/mm)			
	PWHS160	PWHS160	PWHS160	PWHS160
Experimental	417	417	417	417
Analytical (loose cable assumption) [Analytical / Experimental stiffness]	358 [0.86]	358 [0.86]	358 [0.86]	358 [0.86]

2900 mm high with plan dimensions of 2650 mm×2150 mm (length by width). The four perimeter columns have welded square hollow sections (150 mm×150 mm×15 mm), while the four beams have hot-formed square hollow sections (120 mm×120 mm×12.5 mm). The base of the structure is characterized by a horizontal braced steel frame (see red elements of Fig. 5(b)), consisting of HEM160 profiles and40 additional concrete blocks (each of size 150 mm×235 mm×305 mm) for a total mass of 2.85 tons. Pin connections are provided between the columns and the beams. The roof supports a reinforced concrete slab having a thickness of 250 mm and a weight of 4.1 tons. The global mass of the base floor is 3.6 tons, and the total mass of the superstructure is 5.35 tons.

The instruments used to monitor the structural response are described in Fig. 5(a), together with a view of the prototype scaled structure in Fig. 5(b). Seven laser displacement transducers (LDSs), model CP35MHT80 (Wenglor Sensoric GmbH, Germany), having capacity ±150 mm and resolution 50µm, were mounted on an external reference frame with respect to the shaking table. Two additional laser transducers (Micro-Epsilon Messtechnik GmbH, Germany), characterized by a capacity of ±300mm and a resolution of 80µm, were mounted to measure the rocking of the frame. Six triaxial piezoelectric acceleration sensors, model 356A17 (PCB Piezotronics Inc., NY) were used to record the absolute accelerations of the masses at different levels. A sampling frequency of 500 Hz was assumed to measure the above quantities, and a filter at 50 Hz was then applied.

3.2 Selection of the ground motions

In accordance with the Italian Seismic Code (ISC) (DM 17 gennaio 2018), seven accelerograms were chosen from the European strong motion database (Iervolino *et al*. 2010) by running REXEL v3.4 beta (Ambraseys *et al*. 2002). The obtained selection represents moderate to high seismic regions in Italy. The design spectrum was obtained from the ISC's guidelines for the life safety limit state of a strategic structure: location in Naples (Italy - 14.2767° longitude, 40.863° latitude), functional class IV (DM 17 gennaio 2018), soil type A, nominal life of 100 years (corresponding to a return period of 1898 years). Ground motions were selected among events with a magnitude (M_w) from 5.3 to 7.3 and a distance from the epicenter (R_{ep}) from 0 to 80 km. The average spectrum of the selected seismic events, in the

Table 5 Selected ground motion parameters

							Full scale earthquake			Scaled earthquake (S_L = 1/3)			
Record	Waveform ID	Station ID	Date [dd/mm/yy]	SF	Mw	R [km]	PGA [m/s^2]	PGV [cm/s]	PGD [cm]	PGA [m/s^2]	PGV [cm/s]	PGD [cm]	HI [mm]
Bingol (BIN)	7142ya	ST539	01/05/2003	0,87	6,3	14	2,55	18,29	3,25	2,55	10,56	1,08	337
Friuli (FRI)	55xa	ST20	06/05/1976	0,72	6,5	23	2,55	15,25	9,29	2,55	8,80	3,10	233
Montenegro (MON)	200ya	ST68	15/04/1979	1,01	6,9	65	2,55	12,87	9,60	2,55	7,43	3,20	206
Etolia (ETO)	428ya	ST169	18/05/1988	1,47	5,3	23	2,55	12,46	6,06	2,55	7,19	2,02	204
Lazio Abruzzo (LAZ)	372ya	ST274	07/05/1984	2,06	5,9	68	2,55	15,02	6,80	2,55	8,67	2,27	172
Campano Lucano (CAM)	290ya	ST96	23/11/1980	0,80	6,9	32	2,55	44,10	16,20	2,55	25,46	5,40	1010
Campano Lucano (CAT)	287ya	ST93	23/11/1980	1,43	6,9	23	2,55	43,90	14,00	2,55	25,35	4,67	854
			mean	1,19	6,4	35							

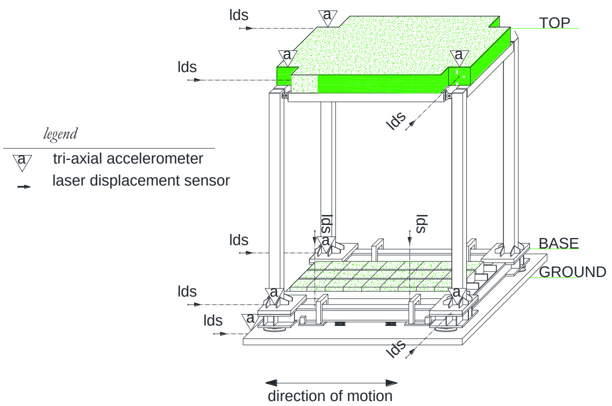

(a)

(b)

Fig. 5 (a) Sketch of the tested frame and the experimental set-up; (b) tested structure on the shaking table

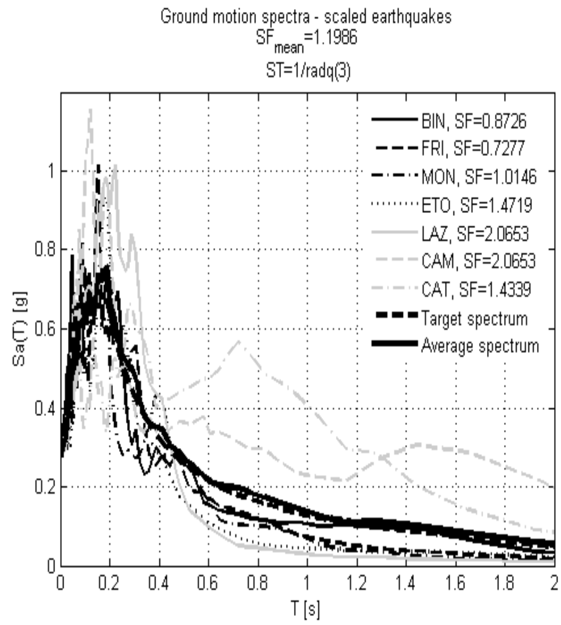

Fig. 6 Scaled ground motion spectra and target spectrum

period range 0.25 - 2s, is able to match the ISC spectrum with a ±10% tolerance. Being the geometry scale factor S_L=1/3 and given an elastic moduli scale factor S_E=1, in order to satisfy the dynamic similitude requirements, the selected earthquakes were compressed in time by a time scale S_T=1/√3. Fig. 6 shows the 5% damped spectra of the selected events. The average scale factor (SF_{mean}) is nearly 1, while the maximum scale factor (SF_{max}) is almost 2. Table 5 reports the characteristics of the unscaled earthquakes and those of the scaled ones. Among the different seismic events, the Campano Lucano 290ya (CAM) accelerogram is characterized by the highest Housner Intensity (HI). The HI is a measure of the damaging power of a seismic event over a wide range of periods (Housner 1975).

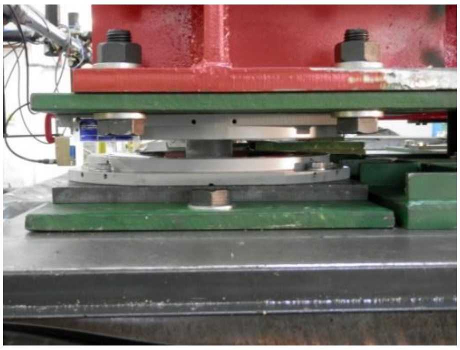

(a)

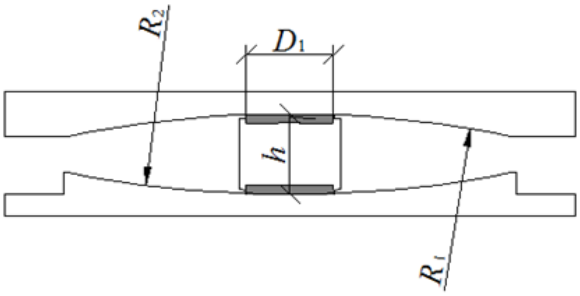

(b)

Fig. 7 Configuration #1_CSS: CSS (a) and most important features (b)

(a)

(b)

Fig. 8 Testing configuration #2_CSS+WR: WRs (a) and their mode of deformation (b)

3.3 Isolation system of the prototype structure

Two different BI systems were tested on a shaking table. In configuration #1_CSSs, the isolation system consisted of 4 CSSs, as shown in Fig. 7(a). Each bearing consists of a lower and an upper concave plate having a 360 mm diameter, and a rigid slider 55mm high (see h in Fig. 7(b)) in intermediate position; the curved sliding surfaces have $R_1 = R_2 = 770$ mm, with effective radius $R_{eff} = R_1 + R_2 - h = 1485$mm (Hussaini *et al.* 1994). The plates' concave sliding surfaces are lined with two sheets of stainless steel, 2.5mm thick. The slider's convex surfaces are lined with two pads of lubricated polytetrafluoroethylene (PTFE), with 60mm diameter and 6 mm thickness. The nominal friction coefficient μ is equal to 0.04, under the pressure level produced by the structural load. The isolator's natural period is T_b=2.45s (related to 1.412s at the scale of the model) and its displacement capacity is $\pm 260\ mm$. The total vertical load is 80.4kN, and the horizontal stiffness K_r of the whole isolation system is 54.4 kN/m.

The testing configuration #2_CSSs+WRs is characterized by the combination of the CSSs mounted in parallel with four WRs. One side of each WR is fixed to the shake table, the other side is firmly linked to the horizontal frame at the base of the tested structure. As clear from Fig. 8, the WRDs are deformed in "shear" during testing.

Fig. 9(a) shows the main coil dimensions of the WR, namely the height h=85 mm, the width v=110 mm and the radius of the individual cable of 3.5mm. Figs. 9(b) and 9(c) show the experimental force - displacement response

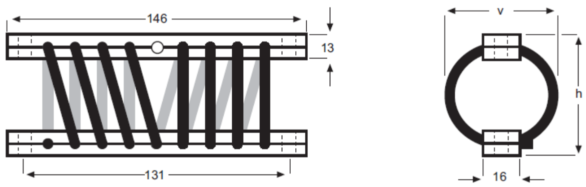

(a)

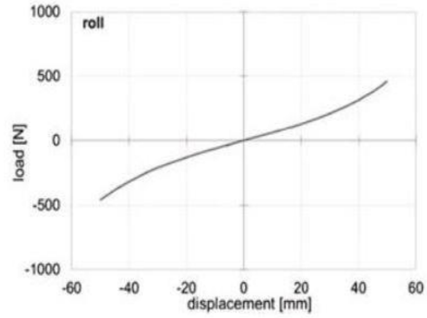

(b)

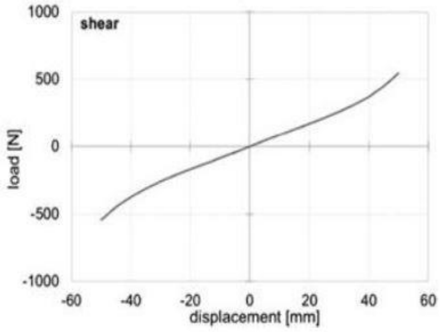

(c)

Fig. 9 Wire-rope device installed in the isolation system: geometrical details (a), "roll" (b) and "shear" (c) modes of deformation

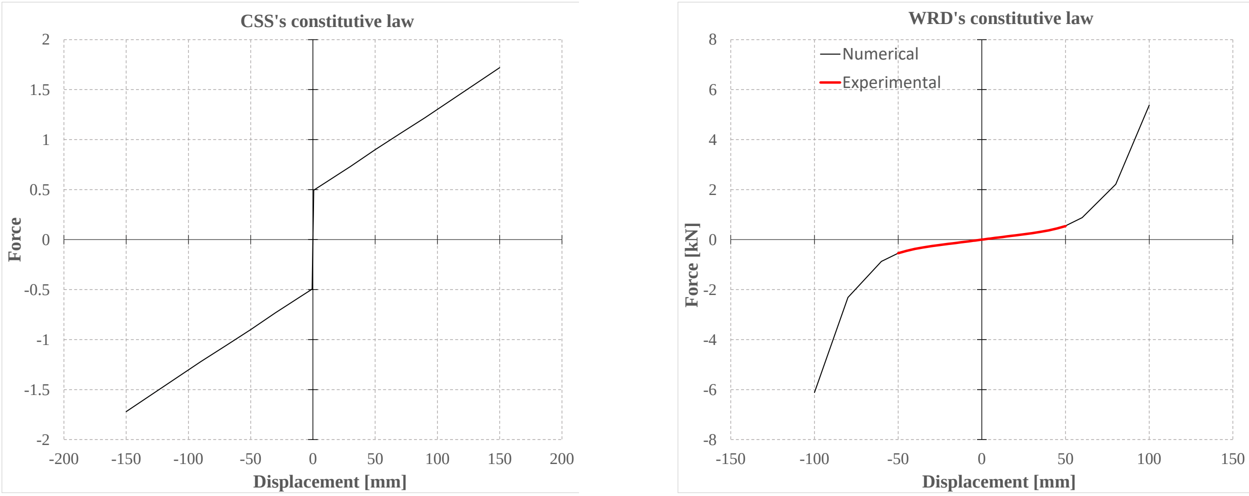

Fig. 10 Force - displacement constitutive law for CSS and WR devices

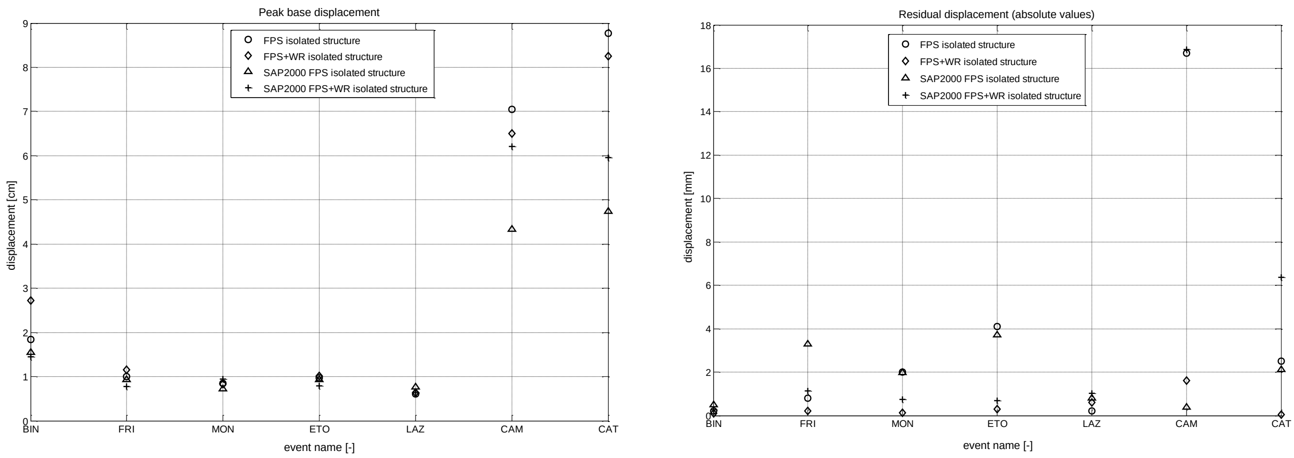

Fig. 11 Base isolated structure: peak base horizontal displacements and residual displacements

obtained from characterization tests carried out along the two horizontal loading directions of the WR. In "shear" and "roll" (Figs. 9(b) and 9(c)), the force displacement response is symmetric and linear up to a displacement of 50mm. A maximum displacement d_{max}=50 mm is measured in shear for a force F_{shear}=545N. The stiffnesses of a WR in shear and roll are equal to 10.9kN/m and 9.2kN/m, respectively. The restoring stiffness of the isolation system in configuration #2_CSSs+WRs is given by $K_r + K_s \approx$ 97.8kN/m, which is related to a natural period of T_{bs}=1.817s (this corresponds to a scaled period of 1.049s).

3.4 Description of the numerical model for nonlinear response history analysis

A 3D model of the building was created in SAP2000. For the base isolated model, as the structure is assumed to remain elastic during all the events, Rayleigh damping of 1.5% of critical was assigned in SAP2000 for the period interval of 0.9 T_1 to 1.2T_1, where T_1 is the first period of the base isolated building (Chopra 2007, Powell 2010). The columns of the structure were modelled as fixed to the horizontal base frame, while the top beams were modelled as pinned to the columns. Multilinear elastic elements were used to simulate the response of the WRs. The multilinear response is shown in Fig. 10 (plot on the right hand side). This model neglects the hysteretic response of the WRs. Nevertheless, the nonlinear response of the CSSs was modelled using a bilinear element in SAP2000 (Fig. 10 - plot on the left hand side).

4. Results

In the following section, for both isolated configurations, including curved surface slider bearings without or with additional wire rope devices (#1_CSSs and #2_CSSs+WRs, respectively), the experimental results were compared to the numerical ones. The characteristic strength F_0 = 3.22kN was assumed for the bilinear hysteretic force – displacement law of CSSs.

However, the restoring stiffness of arrangement #2_CSSs+WRs resulted equal to 97.8kN/m, i.e. approximately twice than that of arrangement #1_CSSs(54.4kN/m), because of the presence of the additional wire

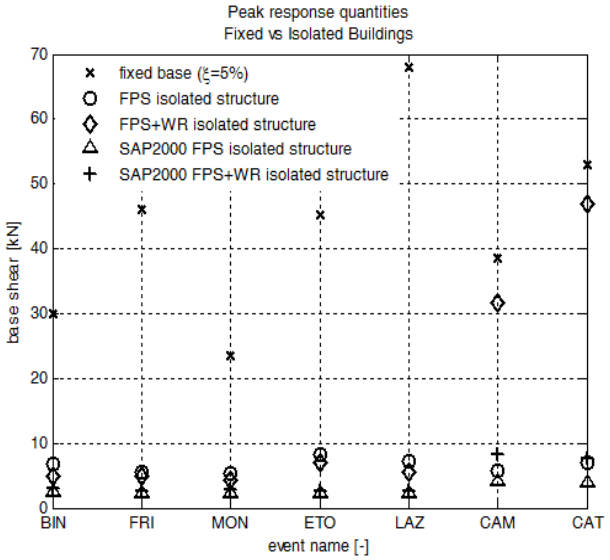

Fig. 12 Base shear

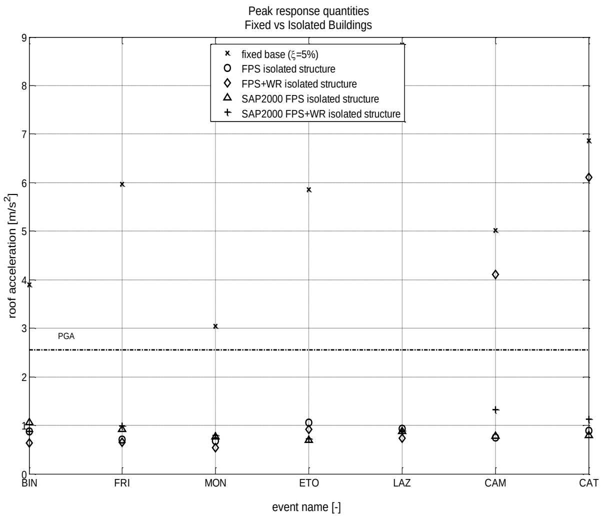

Fig. 13 Isolated building versus 5% damped structure, in terms of peak roof accelerations

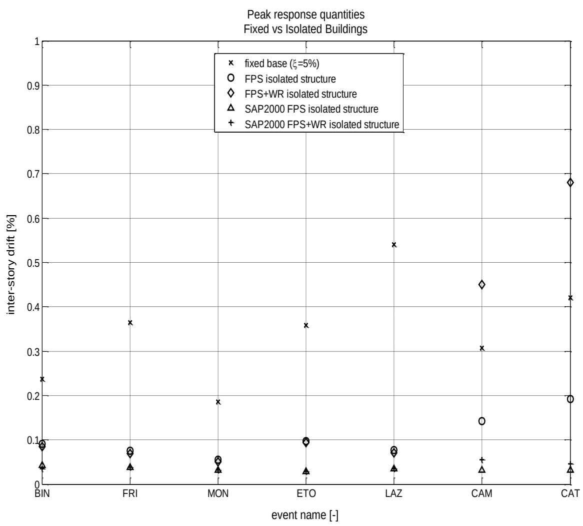

Fig. 14 Peak values of interstory drift

rope elements. The corresponding values of the static residual displacement are d'_{rm}=33 mm in configuration #2_FPS+WR and d_{rm}=59 mm in configuration #1_FPS.

During the tests performed on configuration 1_CSSs, a considerable residual displacement was recorded in comparison with the peak transient displacement, after ETO, MON, CAM and CAT earthquakes. At the end of the tests carried out with arrangement #2_CSSs+WRs, no residual displacements were detected, that is, an enhancement in the system's re-centering capability was observed (see next Fig. 11). The base shear is plotted in Fig. 12 for the isolated structure as well as for the 5% damped fixed base structure. For all structural configurations, that is fixed base and base isolated, the peak accelerations in both the arrangements (#1_CSSs and #2_CSSs+WRs) at top level, and the peak inter-story drifts are compared in Figs. 13 and 14.

The peak horizontal displacements (Fig. 11) never exceeded the linear deformation range of WRs, except under the strong ground motions CAM and CAT. Under moderate inputs, the WRs offered a negligible contribution to the modification of the response of the isolation system during the strong motion phase, and the system's maximum transient displacement was not modified significantly by the WRs. However, the wire rope devices had a relevant effect during the coda phase, thanks to their restoring action and their effectiveness in reducing the residual displacement (see MON and ETO events in Fig. 11). Due to the large horizontal displacements exhibited under CAM and CAT records, the wire rope devices' deformations exceeded the linear range, which corresponds to a consistent increase of the stiffness; however, their presence in the second configuration caused the complete re-centering of the base isolation system at the end of the shaking produced by the above mentioned strong earthquakes. It is also worth to point out that, after the experiments, no visual signs of degradation or damage were detected in the wire rope springs. The comparison of configuration #2_CSSs+WRs with #1_CSSs underlined a considerable increase of the base shear in configuration #2_CSSs+WRs, under CAM and CAT strong motions (see Fig. 12), due to the effect of the increased stiffness determined by larger displacements: while the maximum displacements decrease of approximately 10% in configuration #2_CSSs+WRs, the shear force normalized with respect to the vertical load rises from 0.075 to the value 0.40 and from 0.087 to 0.58, respectively under CAM and CAT seismic inputs. Accordingly, during CAM and CAT accelerograms, the second isolation system configuration was not helpful in reducing the accelerations transmitted to the upper structure from the shaking table (Fig. 13): during these seismic excitations, the increase of stiffness caused by excessive displacements produces a decrease of the effective vibration period of the isolated structure, therefore amplifying the accelerations, while, in the fixed base structure, significant accelerations were detected during six out of the seven earthquake records. Therefore, during the CAM and CAT seismic excitations, the experimental response of the tested structure isolated by means of sliders + wire ropes became only slightly lower than the numerical response of the fixed

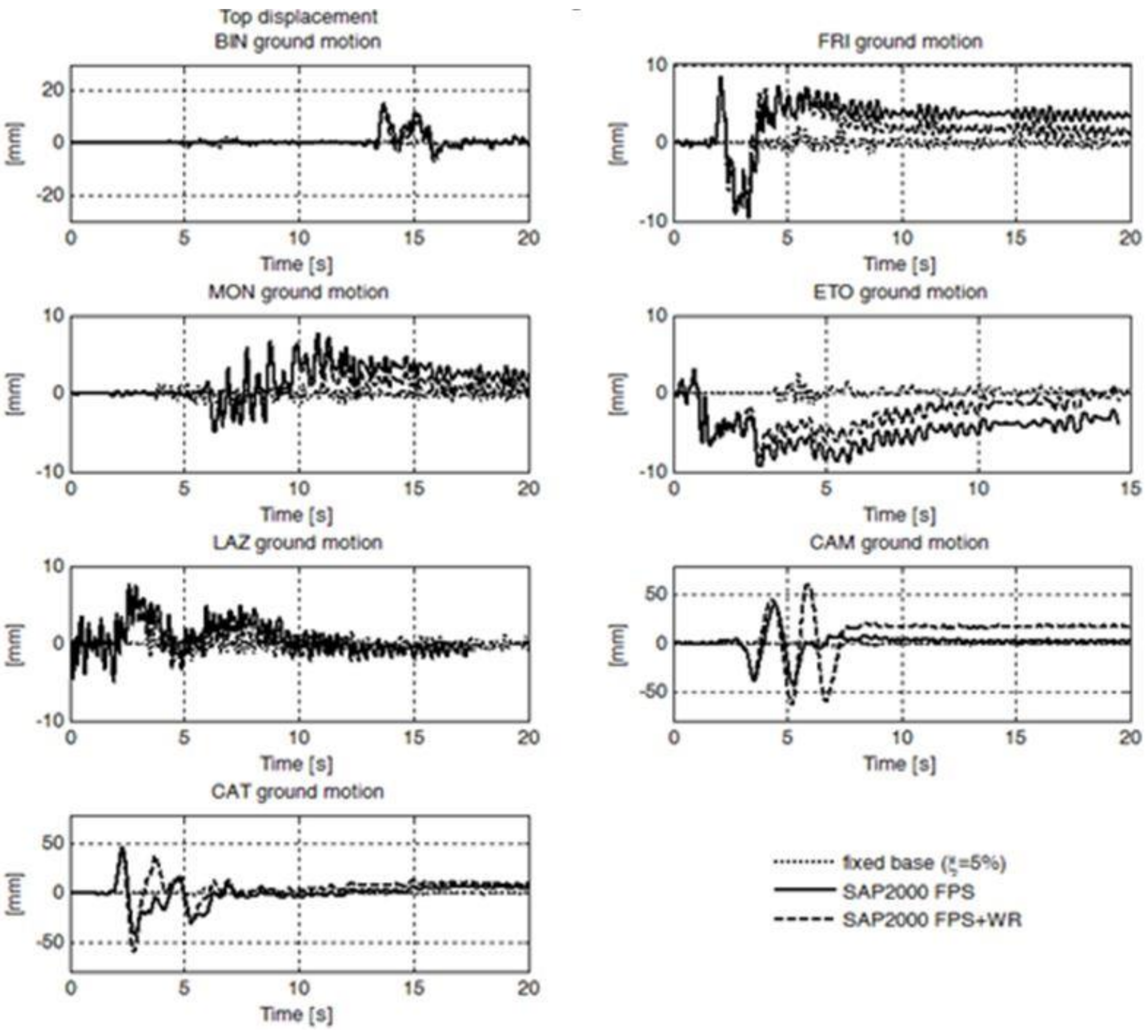

Fig. 15 Top displacement versus time

base structure, both in terms of peak roof accelerations and shear forces. Finally, Fig. 14 shows the comparisons in terms of experimental peak interstory drifts, while Fig. 15 presents the top displacement time histories for the fixed base structure and for both configurations #1_CSSs and #2_CSSs+WRs.

The discussed experimental results demonstrated both the applicability of WRs as auxiliary re-centering devices in seismic isolation systems and the importance of the devices' complete characterization of their force – displacement constitutive laws. As regard the latter issue, further experiments should be performed with the devices working in the non-linear range on a full-scale structure.

Acknowledgments

The authors would like to acknowledge the support of the Italian Department of Civil Protection (P.E. 2010-2013 - Task 2.3.2 - Development of new technologies for seismic mitigation). They are also grateful for the support provided by Powerflex S.r.l., Limatola (BN), supplier of the wire-rope devices discussed in this study.

References

Ambraseys, N., Smit, P., Sigbjornsson, R., Suhadolc, P. and Margaris, B. (2002), "Internet-Site for European Strong-Motion Data", European Commission, Research-Directorate General, Environment and Climate Program 2002, http://www.isesd.hi.is/ESD_Local/frameset.htm [24 July 2013].

Belluzzi, O. (1966), *Science of the Constructions*, Zanichelli, Bologna, Italy.

Calabrese, A., Spizzuoco, M., Serino, G., Della Corte, G. and Maddaloni, G. (2015), "Shake table investigation of a novel, low-cost, base isolation technology using recycled rubber", *Struct. Health Monit.*, **22**(1), 107-122, http://:10.1002/stc.1663.NTC.

Cardone, D., Gesualdi, G. and Brancato, P. (2015), "Restoring capability of friction pendulum seismic isolation systems", *Bull. Earthq. Eng.,* http://10.1007/s10518-014-9719-5.

Chopra, A.K. (2007), *Dynamics of Structures: Theory and applications to earthquake engineering*, Prentice-Hall, Englewood Cliffs, N.J. U.S.A.

Costello, G.A. (1990), *Theory of Wire Rope*, (4th Edition), Springer Verlag, New York. U.S.A.

Cutchins, M.A., Cochran, J.E., Kumar, K., Fitz-Coy, N.G. and Tinker, M.L. (1987), Initial investigations into the damping characteristics of wire rope vibration isolators, Final Technical Report prepared under NASA Research Grant NAG8-532, Engineering Experiment Station, Auburn University, Alabama.

Demetriades, G.F., Costantinou, M.C. and Reinhorn, A.M. (1993), "Study of wire rope systems for seismic protection of equipment in buildings", *Eng. Struct.*, **15**(5), 321-334. https://doi.org/10.1016/0141-0296(93)90036-4.

Den Hartog, J.P. (1961), *Strength of Materials*, Dover Publications Inc, New York. U.S.A.

Di Donna, M. and Serino, G. (2002), "Base isolation of high-voltage equipment: comparison between two different solutions", *Proc. of the 7th International Conference on Probabilistic Methods Applied to Power Systems*, Napoli, Italy.

Dolce, M., Cardone, D. and Croatto, F. (2005), "Frictional behavior of steel-PTFE interfaces for seismic isolation", *Bull. Earthq. Eng.*, **3**(1), 75-99. https://doi.org/10.1007/s10518-005-0187-9.

Gesualdo, F.A.R. and Lima, M.C.V. (2012), "An initial investigation of the inverted trussed beam formed by wooden rectangular cross section enlaced with wire rope", *Struct. Eng. Mech.*, **44**(2), 239-255, http://dx.doi.org/10.12989/sem.2012.44.2.239.

Ghalandari, A., Ghasemi, M.R. and Dizangian, B. (2018), "Enhancing seismic performance of ductile moment frames with delayed wire-rope bracing using middle steel plate", *Steel Compos. Struct.*, **28**(2), 139-147, http://dx.doi.org/10.12989/scs.2018.28.2.139.

Giannini, R., Alessandri, S., Paolacci, F. and Malena, M. (2015), "Seismic retrofitting of a HV circuit breaker through base isolation with steel cable dampers. Part 1: Preliminary tests and analyses", *Eng. Struct.*, http://10.1016/j.engstruct.2015.03.032.

Housner, G.W. (1975), "Measures of severity of earthquake ground shaking", *Proceedings of the U.S. National Conference on Earthquake Engineering*, Ann Arbor, Miami. U.S.A.

Hussaini, T.M., Zayas, V.A. and Constantinou, M.C. (1994), Seismic isolation of a multi-story frame structure using spherical sliding isolation systems, Technical Report No. NCEER-94-0007, National Center for Earthquake Engineering Research, Buffalo, N.Y. U.S.A.

Iervolino, I., Galasso, C. and Cosenza, E. (2010), "REXEL: computer aided record selection for code - based seismic structural analysis", *Bull. Earthq. Eng.*, **8**(2), 399-362, https://doi.org/10.1007/s10518-009-9146-1.

Ismail, M., Rodellar, J. and Pozo, F. (2016), "An isolation device for near-fault ground motions", *Struct. Health Monit.*, **21**(3), 249-268. https://doi.org/10.1002/stc.1549.

Katsaras, C.P., Panagiotakos, T.B. and Kolias, B. (2008), "Restoring capability of bilinear hysteretic seismic isolation system", *Earthq. Eng. Struct. Dyn.*, **37**(4), 557-575. https://doi.org/10.1002/eqe.772.

Liossatou, E. and Fardis, M.N. (2016), "Near-fault effects on residual displacements of RC structures", *Earthq. Eng. Struct. Dyn.*, **45**(9), 1391-1409, https://doi.org/10.1002/eqe.2712.

Love, A.E.H. (1927), *A Treatise on the Mathematical Theory of Elasticity,* Dover Publications, New York. U.S.A.

Nuove norme tecniche per le costruzioni. DM 17 gennaio 2018, Circolare 21 gennaio 2019 n. 7 C.S.LL.PP., Gazzetta Ufficiale n. 42 del 29 febbraio 2018 - Supplemento Ordinario n. 30. http://www.cslp.it/cslp/index.php?option=com_docman&task=doc_download&gid=3269&Itemid=10 [24 July 2013] (in Italian).

Powell, G.H. (2010), *Modeling for structural analysis: behavior and basics*, Computers and Structures, Inc., Berkeley, California, U.S.A.

Quaglini, V., Dubini, P. and Poggi, C. (2012), "Experimental assessment of sliding materials for seismic isolation systems", *Bull. Earthq. Eng.*, **10**(2), 717-740. https://doi.org/10.1007/s10518-011-9308-9.

Quaglini, V., Gandelli, E. and Dubini, P. (2017), "Experimental investigation of the recentring capability of curved surface sliders", *Struct. Health Monit.*, **24**(2), e1870, https://doi.org/10.1002/stc.1870.

Serino, G., Bonacina, G. and Bettinali, F. (1995), "Passive protection devices for high-voltage equipment: design procedures and performance evaluation", *Proceedings. of the 4th US Conference Sponsored by the ASCE Technical Council on Lifeline Earthquake Engineering*, San Francisco, California,

Spizzuoco, M., Quaglini, V., Calabrese, A., Serino, G. and Zambrano, C. (2017), "Study of wire rope devices for improving the re-centering capability of base isolated buildings", *Struct. Health Monit.*, **24**(6), 1-16. https://doi.org/10.1002/stc.1928.

Vaiana, N., Spizzuoco, M. and Serino, G. (2017a), "Wire rope isolators for seismically base-isolated lightweight structures: experimental characterization and mathematical modeling", *Eng. Struct.*, **140**, 498-514, http://dx.doi.org/10.1016/j.engstruct.2017.02.057.

Vaiana, N., Spizzuoco, M. and Serino, G. (2017b), "A parallel model for predicting the horizontal dynamic behavior of helical wire rope isolators", *Int. J. Civil Struct. Eng.*, **4**(1), 63-68, ISSN 2372-3971.

Yurdakul, M. and Ates, S. (2011), "Modeling of triple concave friction pendulum bearings for seismic isolation of buildings", *Struct. Eng. Mech.*, **40**(3), https://doi.org/10.12989/sem.2011.40.3.315.

CC